Steitz, T. A., & Shulman, R. G. (1982) *Annu. Rev. Biophys. Bioeng. 11*, 419-444.
Still, W. C., Kahn, M., & Mitra, A. (1978) *J. Org. Chem. 42*, 2923-2925.
Stroud, R. M., Kay, L. M., & Dickerson, R. E. (1974) *J. Mol. Biol. 83*, 185-208.
Takahashi, L. H., Radhakrishnan, R., Rosenfield, R. E., Jr., Meyer, E. F., Jr., & Trainor, D. A. (1989a) *J. Am. Chem. Soc. 111*, 3368-3374.
Takahashi, L. H., Radhakrishnan, R., Rosenfield, R. E., Jr., & Meyer, E. F., Jr. (1989b) *Biochemistry 28*, 7610-7617.
Thompson, R. C., & Blout, E. R. (1973) *Biochemistry 12*, 51-57.
Thompson, R. C., & Bauer, C. A. (1979) *Biochemistry 18*, 1552-1558.
Van der Drift, A. C. M., Beck, H. C., Dekker, W. H., Hulst, A. G., & Wils, E. R. (1985) *Biochemistry 24*, 6894-6903.
Visser, L., & Blout, E. R. (1972) *Biochem. Biophys. Res. Commun. 268*, 257-260.
Westheimer, F. H. (1968) *Acc. Chem. Res. 1*, 70-78.

Crystal Structures of α-Lytic Protease Complexes with Irreversibly Bound Phosphonate Esters[†,‡]

Roger Bone,[§,∥] Nicole S. Sampson,[⊥] Paul A. Bartlett,[⊥] and David A. Agard[*,§]

Department of Biochemistry and Biophysics and The Howard Hughes Medical Institute, University of California at San Francisco, San Francisco, California 94143-0448, and Department of Chemistry, University of California at Berkeley, Berkeley, California 94720

Received June 29, 1990; Revised Manuscript Received October 29, 1990

ABSTRACT: The structures of the complexes with α-lytic protease of both phosphorus stereoisomers of *N*-[(2*S*)-2-[[[(1*R*)-1-[*N*-[(*tert*-butyloxycarbonyl)-L-alanyl-L-alanyl-L-prolyl]amino]-2-methylpropyl]-phenoxyphosphinyl]oxy]propanoyl]-L-alanine methyl ester, an analogue of the peptide Boc-Ala-Ala-Pro-Val-Ala-Ala where Val is replaced with an analogous phosphonate phenyl ester and the subsequent Ala is replaced with lactate, have been determined to high resolution (1.9 Å) by X-ray crystallography. Both stereoisomers inactivate the enzyme but differ by a factor of 2 in the second-order rate constant for inactivation [Sampson, N. S., & Bartlett, P. A. (1991) *Biochemistry* (preceding paper in this issue)]. One isomer (B) forms a tetrahedral adduct in which the phosphonate phenyl ester is displaced by the active site serine (S195) and interacts with the enzyme across seven substrate recognition sites that span both sides of the scissile bond. Seven hydrogen bonds are formed with the enzyme, and 510 Å^2 of hydrophobic surface area is buried when the inhibitor interacts with the enzyme. Although two hydrogen bonds are gained by incorporation of two residues on the C-terminal side of the scissile bond into the inhibitor, there is very little adjustment in the structure of the enzyme in this region. Surprisingly, the active site histidine (H57) does not interact with the phosphonate, apparently because the phosphonate lacks negative charge in or near the oxyanion hole, and instead, the side chain rotates out of the active site cleft and hydrogen bonds with solvent. The other isomer (A) forms a mixture of two different tetrahedral adducts in the active site, both covalently bonded to Ser 195. One adduct, at approximately 58% occupancy, is exactly the same in structure as the complex formed with isomer B, and the other adduct, at 42% occupancy, has lost the two residues C-terminal to the scissile bond by hydrolysis. In the lower occupancy structure, His 57 does not rotate out of the active site and forms a hydrogen bond with the phosphonate oxygen instead. The structures of both complexes were insensitive to pH. As very little change in structure accompanies the histidine rotation, the complex with isomer B provides an excellent mimic for the structure of the transition state (or high-energy reaction intermediate) that spans both sides of the scissile bond.

To provide an understanding for the structural basis of serine protease catalysis, the structures of many serine proteases in the absence and presence of various types of inhibitors have been determined by X-ray crystallography. Three structures are of the greatest interest: the structure of the free enzyme, the structures of complexes with substrate analogues, and the structures of complexes with transition-state analogues and/or with analogues of reaction intermediates. These structures reveal how the enzyme interacts with substrates, how those interactions change during the transition state, and whether conformational changes are required in order to accommodate substrates. The structures of numerous unliganded serine proteases have been determined by crystallography, including α-lytic protease (Fujinaga et al., 1985; Brayer et al., 1979b), chymotrypsin (Blow, 1976; Tsukada & Blow, 1984; Blevins & Tulinsky, 1985), elastase (Meyer et al., 1988), proteinase A (*Streptomyces griseus*; Brayer et al., 1978a,b; Seilecki et al., 1979), several trypsins (Walter et al., 1982; Marquart et al., 1983; Read & James, 1988), and subtilisins (Alden et al., 1971; Drenth et al., 1972). These structures provide a basis

[†] This work was supported by funds from the Howard Hughes Medical Institute and from an NSF Presidential Young Investigator grant (D.A.A.) and an NSF Predoctoral Fellowship to N.S.S.
[‡] Crystallographic coordinates of the complexes of α-lytic protease with phosphonates A and B have been deposited in the Protein Data Bank.
* Author to whom correspondence should be addressed.
[§] University of California, San Francisco.
[∥] Current address: Department of Biophysical Chemistry, Merck Sharp & Dohme Research Laboratories, Box 2000 (RY80M-136), Rahway, NJ 07065.
[⊥] University of California, Berkeley.

0006-2960/91/0430-2263$02.50/0

Chart I

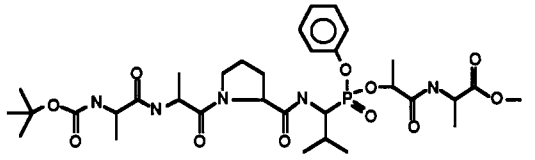

Boc-Ala-Ala-Pro-(OPh)Pval-Lac-Ala-OMe

for understanding serine protease mechanism and for interpreting structural changes that occur as a result of ligand binding. Studies of the structures of complexes between serine proteases and peptide product inhibitors (Walter et al., 1982; Meyer et al., 1986; James et al., 1980) or protein inhibitors (McPhalen & James, 1988; Bode et al., 1987, 1989; Fujinaga et al., 1982, 1987; Read et al., 1983; Seilecki et al., 1983; Read & James, 1988; Marquart et al., 1983) have revealed how substrates interact with these enzymes on both sides of the scissile bond, but in the ground state or Michaelis complex. For serine proteases the transition state is believed to be near in structure to a high-energy, anionic, tetrahedral intermediate that is formed when Ser 195 attacks the carbonyl carbon of the scissile bond. Peptidyl aldehydes, boronic acids, and other compounds mimic formation of high-energy tetrahedral intermediates by forming stable adducts with the active site Ser and have been studied by X-ray crystallography (Thompson, 1983; Brayer et al., 1979a; Delbaere & Brayer, 1985, 1980; James et al., 1980; Kettner & Shenvi, 1984; Kettner et al., 1987; Bone et al., 1987, 1989b; Tulinsky & Blevins, 1987; Matthews et al., 1975; R. Bone, C. A. Kettner, and D. A. Agard, unpublished results; Stroud et al., 1974a,b; Chambers & Stroud, 1977). These structures are excellent mimics of the transition state but only provide information regarding how residues to the amino-terminal side of the scissile bond interact with the enzyme during the transition state. Fluoroketones offer the possibility of incorporating residues C-terminal to the scissile bond and have been examined structurally in complexes with elastase (Imperiali & Abeles, 1986; Takahashi, et al., 1989), but to date, the structures studied have not included good analogues of the P_1' and P_2' residues.[1] Absent is a good image of how substrates interact with serine proteases during the transition state on the carboxy-terminal side of the scissile bond.

Recently, methods have been developed for incorporating phosphonate esters into peptides, creating peptide analogues in which an internal trigonal peptide linkage has been replaced with a tetrahedral phosphonate ester linkage (Sampson & Bartlett, 1988). Phenyl esters of these phosphonates are selective irreversible inactivators of serine proteases in which the phenyl ester is believed to be displaced from the phosphonate by the active site serine (Sampson & Bartlett, 1991). Such irreversible adducts should span both sides of the scissile bond and be excellent mimics of the high-energy tetrahedral reaction intermediate and the transition state. In this work we report the determination by high-resolution X-ray crystallography of the structure of the irreversible complexes formed between α-lytic protease, an extracellular serine protease of *Lysobacter enzymogenes*, and both phosphorus stereoisomers of *N*-[(2*S*)-2-[[[(1*R*)-1-[*N*-[(*tert*-butyloxycarbonyl)-L-alanyl-L-alanyl-L-prolyl]amino]-2-methylpropyl]phenoxyphosphinyl]-oxy]propanoyl]-L-alanine methyl ester, a peptidyl phosphonate diester (phosphonates A and B; see Chart I).

[1] In protease substrate nomenclature the residue to the N-terminal side of the scissile bond is the P_1 residue, the next residue toward the N-terminus is the P_2 residue, etc. (Schecter & Berger, 1967).

Table I: Crystallographic Characterization of Phosphonate Complexes with α-Lytic Protease

complex	pH	resolution (Å)	% rfls ($I/\sigma_I > 3$)	*R* factor	σ_{bonds} (Å)	σ_{angles} (Å)
phosphonate A	8.5	1.93	89	0.127	0.016	0.051
phosphonate A	7.2	2.00	88			
phosphonate A	5.5	2.00	90			
phosphonate B	7.2	1.90	85	0.124	0.017	0.051
phosphonate B	6.0	2.00	92			

Experimental Procedures

Cloned α-lytic protease was purified from culture filtrates of *Escherichia coli* as previously described (Silen et al., 1989; Whitaker, 1970; Hunkapiller et al., 1973) and migrated as a single band when subjected to low-pH native polyacrylamide gel electrophoresis (Hames & Rickwood, 1981). To prepare enzyme–inhibitor complexes, α-lytic protease was dissolved in doubly distilled water (1 mg/mL) and treated with a 3–5-fold excess of phosphonate A or B (5 mM in MeOH)[2] until there was no detectable activity (using succinyl-Ala-Pro-Ala-*p*-Na as a substrate, Peptide Institute). The total time required for inhibition was approximately 2 h. The solution was then successively ultrafiltered and diluted with H_2O at 3 °C in an Amicon Centricon-10 filter (M_r cutoff 10 000) to remove excess inhibitor and concentrated to a final concentration of ca. 20 mg/mL phosphonylated enzyme. This procedure was performed separately with diastereomers A and B.

Crystallography. Crystals of α-lytic protease–inhibitor complexes were grown from vapor diffusion droplets that were prepared by mixing 5 μL of 1.3 M lithium sulfate, adjusted to pH 7.2 with dilute LiOH and H_2SO_4, and 5 μL of 20 mg/mL α-lytic protease–phosphonate complex. The drops were allowed to equilibrate for 2 days at ambient temperature and were then seeded with small crystals (approximately 25 μm in length) of protease, the seeds being serially diluted through 6 drops. Initially, native seeds were used (Bone et al., 1987; Brayer et al., 1979b) and then seeds of the enzyme–inhibitor complexes. The pH was adjusted by addition of 0.5-μL aliquots of 50 mM H_2SO_4 and determined by dotting mother liquor onto pH indicator sticks (MCB Reagents).

Data from crystals of enzyme–inhibitor complexes were collected from single crystals on a Rigaku AFC5 automated diffractometer, equipped with a graphite monochrometer (Stroud et al., 1974a,b; Wycoff et al., 1967). Additional higher resolution data sets were collected from a second crystal and merged with data from the first crystal. Crystals of enzyme–inhibitor complexes were isomorphous with native crystals and generally had cell parameters that differed by less than 0.75%. The intensities of seven check reflections were monitored in order to correct for crystal decay, which was less than 20% over the course of data collection. Corrections were also made for absorption, Lorentz, and polarization by standard methods and for backgrounds according to Krieger

[2] Abbreviations: mAAP, methoxysuccinyl-Ala-Ala-Pro-; Boc, *tert*-butyloxycarbonyl; Boc-AP, *tert*-butyloxycarbonyl-Ala-Pro-; Tris, tris-(hydroxymethyl)aminomethane; MeOH, methanol; *p*-Na, *p*-nitroanilide; Lac, lactoyl residue; rms, root mean square. The prefix "boro" of boroVal- indicates that the carbonyl of the amino acid residue, in this case a valyl residue, is replaced by $-B(OH)_2$; the systematic name for valine boronic acid would be (1-amino-2-methylpropyl)boronic acid. Phosphonate A and phosphonate B, although their configurations have not been assigned, are the resolved phosphorus stereoisomers of *N*-[(2*S*)-2-[[[(1*R*)-1-[*N*-[(*tert*-butyloxycarbonyl)-L-alanyl-L-alanyl-L-prolyl]-amino]-2-methylpropyl]phenoxyphosphinyl]oxy]propanoyl]-L-alanine methyl ester.

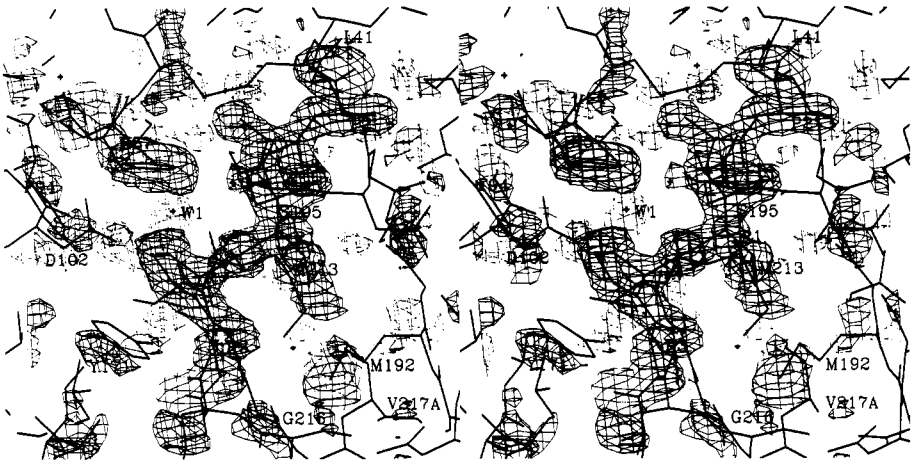

FIGURE 1: Stereo drawing of the difference electron density map ($|F_o| - |F_c|$) for the complex of α-lytic protease and phosphonate B with F_c and ϕ_c calculated from the refined coordinates of native α-lytic protease (Fujinaga et al., 1985) minus the solvent and sulfate that occupy the active site cleft. The long stretch of continuous electron density is interpreted as being the P_4–P_2' residues of the phosphonate. The coordinates displayed are the final refined coordinates for the phosphonate B complex with the enzyme.

Table II: Structural Characterization of Phosphonate Complexes with α-Lytic Protease

E–I complex	rms main-chain deviation (Å)	buried surface area (Å²) total	buried surface area (Å²) hydrophobic
phosphonate A	0.147	610	390
phosphonate B	0.158	810	510
bAP-boroVal	0.130	580	370
mAAP-boroVal	0.143	550	350

et al. (1974). Data were collected by ω-scan in shells of 2θ with the scan rate adjusted so that at least 85% of the reflections had intensities greater than 3σ over the entire data set (Table I).

Initial Fourier maps were computed from the refined coordinates of either α-lytic protease (Fujinaga et al., 1985) without the active site solvent and sulfate or the complex between α-lytic protease and mAAP-boroVal (Bone et al., 1989b) without four active site water molecules and the inhibitor. Maps were inspected, and the inhibitors were placed with the interactive graphics package FRODO (Jones, 1982) after which the coordinates were refined by the stereochemically restrained least-squares algorithm of Hendrickson and Konnert (1981), modified for multiple occupancy refinement (Smith et al., 1988), adapted for use on the FPS 264 array processor (Furey, 1984), and further modified by us. The final overall crystallographic R factors for the comparison of observed and calculated structure factors are listed in Table I. Surface area calculations (Table II) were done with the molecular surfacing program MS (Conolly, 1983a,b).

NMR. ^{31}P NMR spectra were obtained at 160 MHz on a Bruker AM400 series Fourier transform spectrometer equipped with an Aspect 3000 computer. A 90° pulse was used with a 2.4-s delay. The spectra were two-level gate decoupled with a WALTZ sequence. Transients (500–2000) were acquired with 2K data points and a spectral width between 6000 and 9000 Hz in the quadrature detection mode at 21 (±1) °C. Chemical shifts are reported in parts per million, referenced to external trimethyl phosphate, at 3.09 ppm, downfield positive.

α-Lytic protease–phosphonate complexes were filtered through Chelex-100 ion exchange resin (Bio-Rad) and lyophilized, and the residue was redissolved in 0.1 M KCl/D_2O (99.9%; also filtered through Chelex-100) and centrifuged for 10 min in an Eppendorf microcentrifuge. The clear supernatant was transferred to a 5-mm NMR tube. All glassware had been previously soaked in concentrated nitric acid and washed with deionized, distilled water. All deuterated solvents were obtained from Cambridge Isotope Laboratories.

The pH was adjusted on an Acumet 915 pH meter (Fisher Scientific) with 0.1 M DCl (99.5%) or 0.1 M NaOD (99.8%) and in D_2O. The values reported represent the pH meter reading without correction for isotope effect. The pH was measured before and after each NMR run, which was accepted only if there was less than 0.1 unit difference in the pH reading.

RESULTS

Although the two phosphonate diastereomers used to inactivate α-lytic protease were separated by HPLC, the absolute configurations of the two compounds have not been assigned (Sampson & Bartlett, 1991). The two diastereomers will be referred to as phosphonates A and B with the same convention as used in Sampson and Bartlett (1991).

Complex with Phosphonate B. Initial difference electron density maps ($|F_o| - |F_c|$) for the complex between α-lytic protease and phosphonate B, using the coordinates of the unliganded enzyme (Fujinaga et al., 1985), clearly showed that inhibitor was bound by the enzyme at a single site with high occupancy and spanned substrate recognition sites S_5–S_2' (Figure 1). In addition, the map clearly indicated that the side chain of His 57[3] had rotated out of the active site cleft and was replaced by a single water molecule (W1, Figure 1). Also, the terminal methyl of Met 192 rotated 120° from its native position, a change which has been observed previously when the enzyme accommodates Val side chains in the primary specificity pocket (Bone et al., 1987, 1989a,b). Maps calculated with Fourier coefficients ($2|F_o| - |F_c|$) showed continuous electron density stretching between the active site Ser (195 O_γ) and the phosphorus of the inhibitor, indicating that a covalent adduct had formed with the active site Ser. This was corroborated by the bond lengths found on refinement (Table III). On the basis of the shape of the electron density about the phosphorus and bond angles after refinement, the geometry of the adduct was tetrahedral (Table III). No density was observed for the C-terminal methyl ester, and it was concluded that the ester had been hydrolyzed.

Enzyme–Phosphonate B Interactions. Many of the protein–inhibitor interactions that stabilize this complex, par-

[3] Residues in α-lytic protease are numbered by homology with chymotrypsin (Fujinaga et al., 1985) and range from 15A to 244.

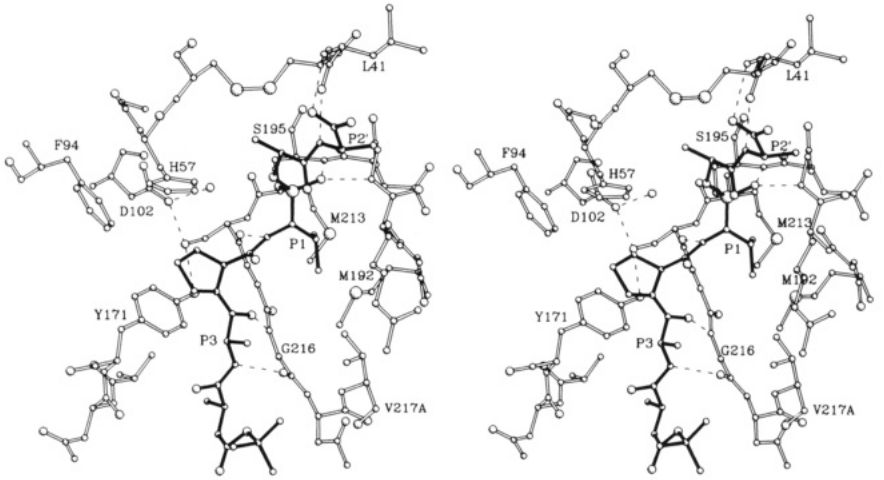

FIGURE 2: Stereo drawing of the active site of the phosphonate B complex with α-lytic protease. Enzyme residues are displayed in open bonds and phosphonate residues in filled bonds, and hydrogen bonds are displayed with dotted lines. The phosphonate is Boc-Ala-Ala-Pro-Pval-Lac-Ala for residues P_5–P_2'.

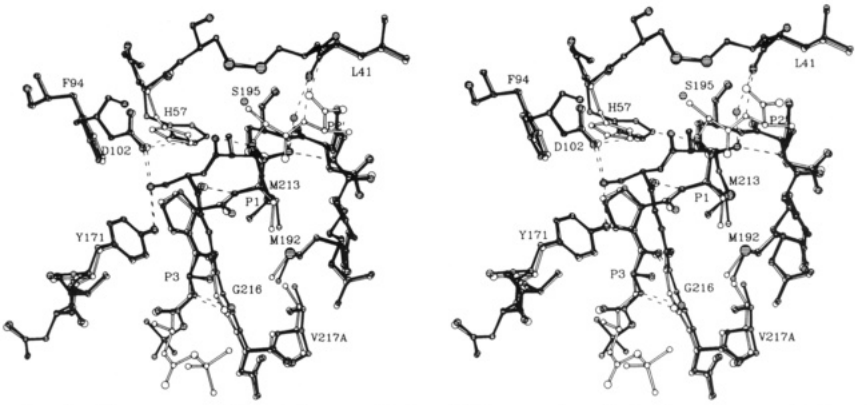

FIGURE 3: Stereo drawing showing the superposition of the coordinates of the complex of α-lytic protease and phosphonate B, in open bonds and atoms, with the coordinates of the complex of α-lytic protease with bAP-boroVal, in filled bonds and shaded atoms. Hydrogen bonds are displayed with dotted lines. The structures are very similar except for the side-chain rotation of His 57.

Table III: Bond Lengths and Angles for Phosphonate Complex

parameter	boronic acid[a]	phosphonate ester[b]	ovomucoid third domain[d]
bond (Å)			
Ser 195 Oγ–P_1 B	1.68	1.55	
P_1 B–P_1 O_1	1.52	1.49	
P_1 B–P_1 O_2	1.49	1.55	
P_1 B–P_1 Cα	1.55	1.61	
bond angle (deg)			
Ser 195 Cβ–Ser 195 Oγ–P_1 B	135	125	
Ser 195 Oγ–P_1 B–P_1 O_1	99	111	
Ser 195 Oγ–P_1 B–P_1 O_2	93	105	
Ser 195 Oγ–P_1 B–P_1 Cα	104	106	
P_1 O_1–P_1 B–P_1 O_2	115	112	
P_1 O_1–P_1 B–P1 Cα	117	113	
P_1 O_2–P_1 B–P1 Cα	111	109	
hydrogen bond (Å)			
Ser 195 N–P_1 O_1	2.9	2.8	3.1
Gly 193 N–P_1 O_1	2.6	2.6	2.6
wat 309 O–P_1 O_1	3.3		
His 57 Nε$_2$–P_1 O_2	2.7	5.5 (2.9[c])	
Ser 214 O–P_1 N	3.0	3.0	3.6
Gly 216 N–Ala P_3 O	3.0	3.0	2.9
Gly 216 O–Ala P_3 N	2.9	2.9	3.0
His 57 Nε$_2$–Ser 195 Oγ	3.0	7.1 (3.0[c])	2.6
Leu 41 O–P_2'N		2.8	2.9
Leu 41 N–P_2'O		3.0	3.1

[a] α-Lytic protease complex with Boc-Ala-Pro-boroVal, taken from Bone et al. (1987). [b] Boc-Ala-Ala-Pro-Pval-Lac-Ala, where Pval is the phosphonic acid analogue of Val and Lac is lactate. [c] Values in the complex with Boc-Ala-Ala-Pro-Pval. [d] Values from Read et al. (1983).

ticularly involving the P_5–P_1 residues, are very similar to those that have been observed to stabilize other serine protease–inhibitor complexes including many α-lytic protease complexes (James et al., 1980; Delbaere & Brayer, 1985; Bone et al., 1987, 1989b). The P_1 phosphonate residue forms three hydrogen bonds with the enzyme, two between the phosphonyl oxygen and the amide protons of Gly 193 and Ser 195 and one between the amide proton and the carbonyl of Ser 214 (Figure 2), and makes van der Waals contacts with the side chains of Met 192, Met 213, and Val 217A and the main chains of residues 214–216 and 192–193 in the primary specificity pocket (Figure 2). These interactions are nearly identical with those made between peptidyl boronic acids and α-lytic protease (Bone et al., 1987, 1989b; Figure 3).

In the P_2 binding site the inhibitor removes hydrophobic surface from solvent by packing of the P_2 Pro against the side chains of Tyr-171, Phe-94, and His-57. The carbonyl and amide protons of the P_3 Ala of the inhibitor make two hydrogen bonds with similar groups on Gly 216 of the enzyme (Figure 2, Table III). These interactions in the P_2 and P_3 binding sites are exactly the same as found in boronic acid complexes with α-lytic protease (Bone et al., 1987, 1989b). Extension of the peptide chain to the P_5 position in the phosphonate creates additional opportunities for removing hydrophobic surface from solvent (Table II) but introduces no new hydrogen bonds. The terminal Boc group is in an unusual conformation in which the carbonyl and NH proton

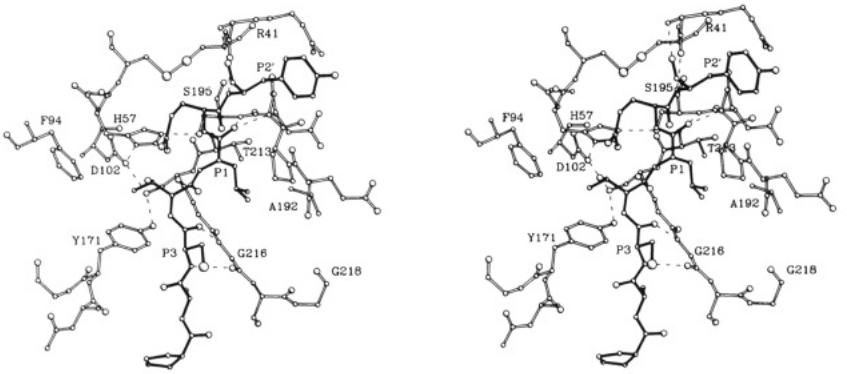

FIGURE 4: Stereo drawing of the complex of *S. griseus* protease B, in open bonds and atoms, with the third domain of turkey ovomucoid, in filled bonds and open atoms, with hydrogen bonds displayed in dotted lines (Read et al., 1983; Fujinaga et al., 1982). The inhibitor is numbered P_5–P_2' by analogy with the phosphonate complex. The true numbers for these residues are 15–19, and the residues are -Pro-Ala-Cys-Val-Leu-Glu-Tyr-. The coordinates were obtained from the Protein Data Bank.

are cis rather than trans and the Boc group extends into solvent, unlike the complex of α-lytic protease with bAP-boroVal (Figure 3). Despite this, the phosphonate complexes bury 40 Å^2 more hydrophobic surface on complex formation than mAAP-boroVal, because of the butyloxycarbonyl group, and 20 Å^2 more than bAP-boroVal, because of the extra Ala residue (compare occupancy A of the phosphonate A complex with values for the boronic acids in Table III).

Extension of the inhibitor to the P_1' and P_2' residues not only adds two hydrogen bonds to the enzyme–inhibitor complex but also contributes an additional 120 Å^2 of buried hydrophobic surface upon complex formation. The hydrogen bonds are formed between the P_2' amide proton and carbonyl and equivalent groups on Leu 41 (Table III). To make these hydrogen bonds, the peptide chain of the inhibitor must cross over and bury the phosphonyl oxygen and leave the P_1' and P_2' Ala side chains projecting toward solvent or solvent-filled channels. In addition, this conformation leaves the phosphonate ester oxygen and the P_1' carbonyl oxygen nearly eclipsed (with a torsional angle of 15°). This conformation is very similar to the conformation adopted by equivalent residues in the third domain of ovomucoid in a complex with SGPB (Read et al., 1983; Fujinaga et al., 1982; Sielecki et al., 1979; Figure 4).

The conformational changes that are induced when phosphonate B reacts with the enzyme are nearly identical with the changes induced when other peptide analogues, such as bAP-boroVal (Bone et al., 1987), bind to the enzyme (Figure 3, Table II). The main-chain atoms of residues 169–175 are shifted away from the active site by a maximum of 0.5 Å, and there are small adjustments in the specificity pocket as in boronic acid complexes. The rms deviation in the positions of main-chain atoms between native and complexed α-lytic proteases are compared in Table II, and the rms main-chain deviation between the complex of α-lytic protease with phosphonate B and the complex with bAP-boroVal is 0.12 Å. The phosphonate B complex has slightly higher deviations than occupancy A in the phosphonate A complex which has deviations nearly equivalent to those of the complex with mAAP-boroVal (Bone et al., 1989b). The phosphonate B complex may have slightly higher deviations due to the change in the histidine position. Of greater interest is that only very small adjustments are observed in the region of Leu 41 as a result of accommodation of the P_1' and P_2' residues (Figure 3).

Complex with Phosphonate A. While difference electron density maps ($|F_o| - |F_c|$), using enzyme–inhibitor complex coordinates (α-lytic protease + mAAP-boroVal; Bone et al., 1989b) without the inhibitor and active site waters, showed that inhibitor was bound in the phosphonate B complex at a single site with high occupancy, they suggested the phosphonate A complex was a mixture of two forms. Initially, the difference maps for the phosphonate A complex suggested that the P_5–P_1 residues of the inhibitor were filled at high occupancy, that a covalent tetrahedral adduct was formed between the P_1 P and Oγ of Ser 195 (Table III), and that His 57 rotated out of the active site. However, electron density for the P_1' and P_2' residues was weak, and it was difficult to identify unambiguously which regions of the map corresponded to the P_2' C_β and COO^-. Following several cycles of restrained refinement, using essentially the same structure as the phosphonate B complex, maps were recalculated with the new model (residues P_5–P_2' present), and negative electron density was observed about residues P_1' and P_2' and positive density in the position occupied by histidine in native enzyme (rotated in). In addition, continued refinement resulted in high temperature factors for the P_1', P_2', and His residues, though electron density returned if the P_1' and P_2' residues were removed for several cycles of refinement. These observations suggested that the enzyme–inhibitor complex was a mixture of two inhibitor forms at nearly equal occupancy, one with the His in a native conformation and one with the His rotated out of the active site. Furthermore, it was concluded that one occupant was identical with the phosphonate B complex (His 57 rotated out), referred to as occupancy B by analogy to the phosphonate B complex, and the other occupant had the ester between the phosphonate and lactate residues cleaved (His 57 native), referred to as occupancy A.

Difference ($|F_o| - |F_c|$) electron density maps were recalculated with the phosphonate A data and the phosphonate B coordinates but with the His 57, W1, and P_5–P_2' residues of the inhibitor set to half-occupancy. These maps revealed residues in positions P_5–P_1, the histidine in its native position, and solvent in the S_1' and S_2' sites (occupancy A revealed; see Figure 6 for a similar map). The structure was refined as a mixture of these two forms, and the occupancies were varied so that the occupancy with the intact phosphonate ester (occupancy B) had temperature factors for residues P_5–P_2' and His 57 equivalent to the values for these residues in the phosphonate B complex.

After refinement a difference map was calculated ($|F_o| - |F_c|$) with phosphonate A complex data and refined coordinates except that the P_1' and P_2' residues were omitted from occupancy B (Figure 5). This map clearly indicates the presence of inhibitor in the S_1' and S_2' sites of the enzyme. In addition, a difference map was calculated by omitting the inhibitor, histidine, and solvents in the S_1' and S_2' sites of occupancy A (Figure 6). This map clearly shows inhibitor in the P_5–P_1

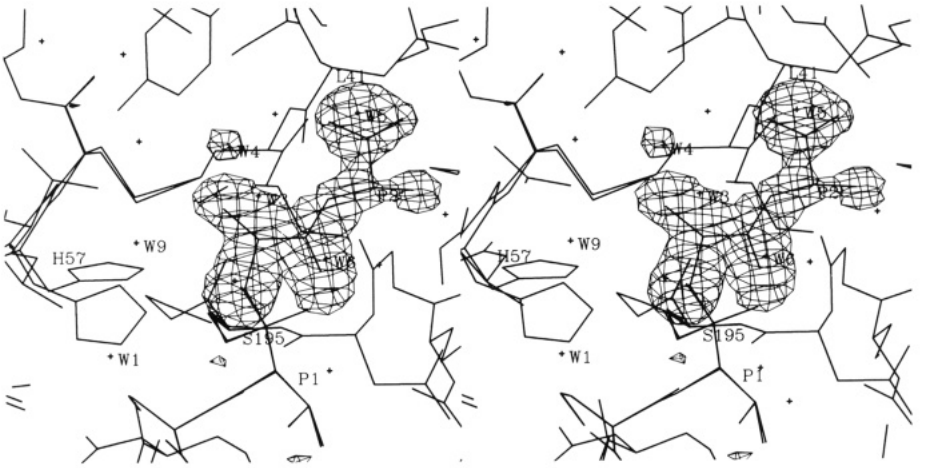

FIGURE 5: Stereo drawing of the difference electron density map ($|F_o| - |F_c|$) for the complex of α-lytic protease and phosphonate A. F_c and ϕ_c were calculated from the final refined coordinates of the phosphonate A complex with the enzyme minus the P_1' and P_2' residues of occupancy B. There is clearly continuous electron density for these residues, indicating they should be included in the structure. The coordinates shown are the final refined coordinates for the complex with both occupancies 1 and 2 displayed.

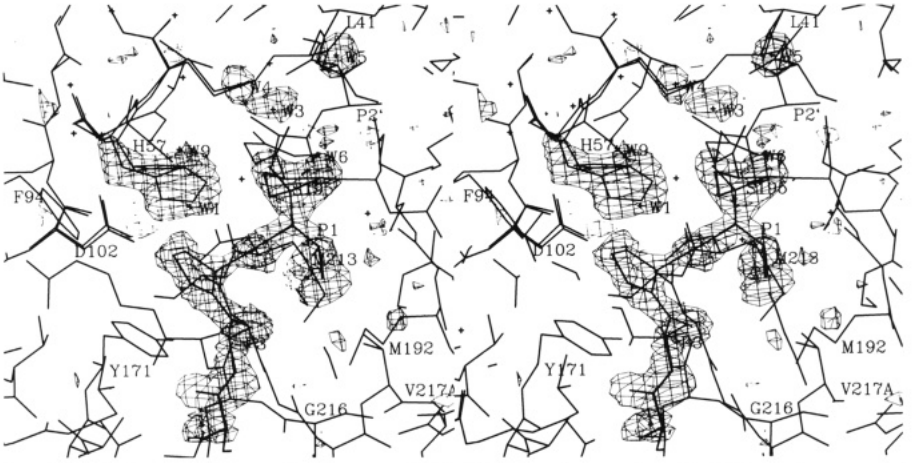

FIGURE 6: Stereo drawing of the difference electron density map ($|F_o| - |F_c|$) for the complex of α-lytic protease and phosphonate A. F_c and ϕ_c were calculated from the final refined coordinates of the phosphonate A complex with the enzyme minus the P_5–P_1 residues, side chain of His 57, and solvents W3–W6 of occupancy A. Clearly, electron density returns for these residues, indicating they should be included in the structure and that the P_1' and P_2' residues should not be present at 100% occupancy. The coordinates shown are the final refined coordinates for the complex with both occupancies 1 and 2 displayed.

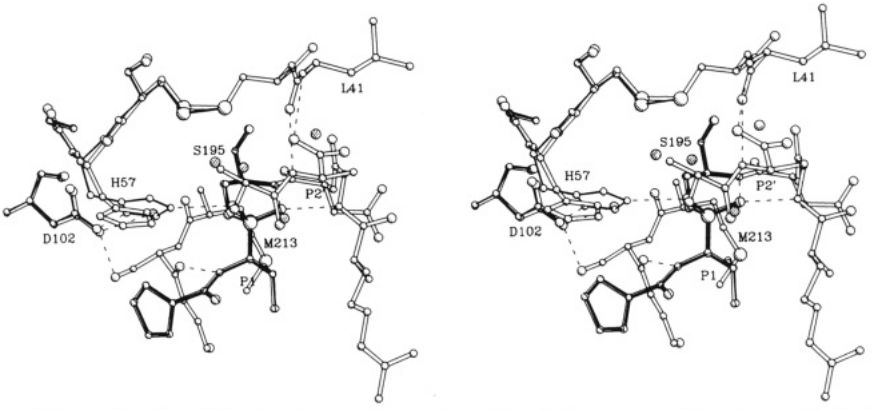

FIGURE 7: Stereo drawing of the active site of the phosphonate 1 complex with α-lytic protease, focusing on the S_1–S_2' substrate recognition sites. Occupancy A is displayed in filled, thin bonds, and occupancy B is displayed in open, wide bonds. The solvents in occupancy A that are alternative to the P_1' and P_2' residues are shaded balls. Hydrogen bonds are displayed with dotted lines.

binding sites, His 57 in its native conformation, and solvent (W3–W6) in the S_1' and S_2' sites (Figure 7). Occupancy B is considered to be identical with the phosphonate B complex while occupancy A is very similar to complexes of the enzyme with boronic acids, having lost all P′ residues.

Enzyme–Phosphonate A Interactions. The structure of residues P_5–P_1 in occupancy A of the phosphonate A complex is nearly identical with the conformation of these residues in either the phosphonate B complex or occupancy B of the phosphonate A complex (assumed to be equivalent). The differences lie in the loss of the P_1' and P_2' residues, their replacement with solvent, and the native conformation of His 57 which allows a hydrogen bond to be formed between $N\epsilon_2$ and the phosphonate oxygen (Table III; Figure 7). Hydro-

gen-bond lengths between this phosphonate and α-lytic protease are almost identical with equivalent hydrogen-bond lengths in the complex with Boc-AP-boroVal (Bone et al., 1987; see Table III). Conformational adjustments are also equivalent. Slightly more hydrophobic surface is removed from solvent when the inhibitor interacts with the enzyme than in the equivalent boronic acid complexes because of the P_5 Boc group or the additional Ala residue.

Histidine Side-Chain Rotation. The most surprising aspect of the structure of the phosphonate B complex, and occupancy B in the phosphonate A complex, is the rotation of the His 57 side chain out of the catalytic triad and into a position in which its hydrogen bonds are satisfied by solvent (Figure 2). The His side chain is replaced by a single molecule of solvent which is hydrogen bonded only to Asp 102. van der Waals contacts with the P_2 proline are nearly equivalent to contacts made in boronic acid complexes in which the His is in a native conformation. However, the position occupied by the phosphonate ester oxygen is not significantly deviant from the position of the corresponding oxygen in boronic acid complexes in which the oxygen hydrogen bonds to the His side chain. There appears to be no steric obstacle to rotation of the His into the active site with formation of a hydrogen bond with the phosphonate oxygen.

One possible explanation for the rotation of His 57 out of the active site in the phosphonate B complex is that it is uncharged and unable to hydrogen bond to the phosphonate oxygen. To test this possibility, the pH was adjusted by addition of 50 mM H_2SO_4 to crystals. When data were recollected at pH 6.0 (original data collected at pH 7.2; Table I) difference electron density maps indicated there was no change in either the His conformation or any other aspect of the structure as the pH was varied. Furthermore, data were also recollected for the phosphonate A complex at pH values of 7.2 and 5.5 (original data at pH 8.5; Table I), and difference maps showed that there was no change in the structure or distribution of the two forms as a function of pH. These results suggest that a positively charged histidine can only be accommodated in a native-like position if there is a negative charge in or near the oxyanion binding pocket. Observations that the positively charged His side chain rotates into solvent when neutrally charged aldehyde adducts are formed with α-lytic protease but not when negatively charged boronic acid adducts or negatively charged product complexes are formed support this conclusion (Brayer et al., 1979a; James et al., 1980; R. Bone, C. A. Kettner, and D. A. Agard, unpublished results; Bone et al., 1987, 1989b).

^{31}P NMR of Enzyme–Inhibitor Complexes. The crystallographic observation of two inhibitor forms in the phosphonate A complex was corroborated by ^{31}P NMR of both enzyme–inhibitor complexes. At pH 5.9 the complex between α-lytic protease and phosphonate A is a mixture of two enzyme-bound species at approximately equal concentrations (δ 20.42 and δ 1.15) while the complex with isomer B contains only one species (δ 1.13). Furthermore, the chemical shift of the complex with isomer B is identical with that of the upfield species present in the complex with phosphonate A.

Using ^{31}P NMR spectroscopy, Markley and co-workers (Porubcan et al., 1979) determined the pK_a of His 57 in α-lytic protease and in (diisopropoxyphosphinyl)-α-lytic protease to be 5.7 and 8.0, respectively. The resonance of the protease complex with phosphonate B titrates with a pK_a value of 6.9, as does the upfield resonance in the spectrum of the complex with isomer A (see Figure 8). In view of the crystallographic results, the upfield resonance represents the hexapeptide

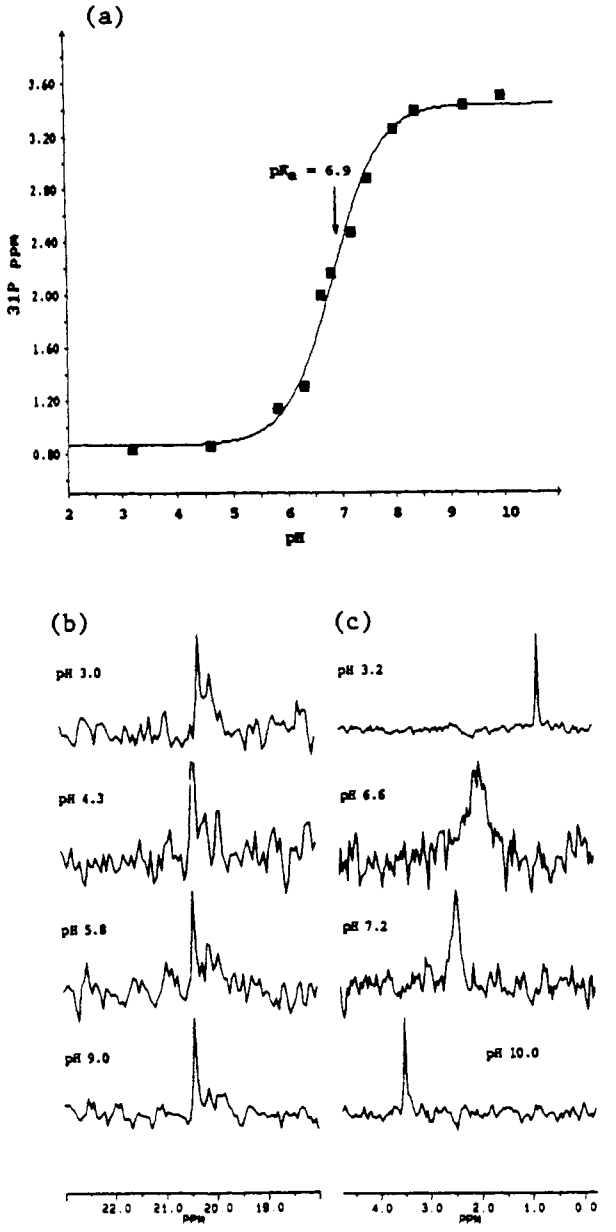

FIGURE 8: 160-MHz ^{31}P NMR spectra and NMR pH titration curve of 0.3 nM solutions of ALP-I(B) ans ALP-I(A) in 0.1 M KCl in ^2H_2O, 21 °C. (a) ^{31}P NMR data for the phosphonate B complex fitted to a theoretical titration curve having a pK of 6.86 (±0.05). (b) Low-field region of ^{31}P NMR spectra of α-lytic protease–phosphonate A. The high-field region of the phosphonate A complex is identical with that of the phosphonate B complex shown in (c). (c) ^{31}P NMR spectra of the α-lytic protease–phosphonate B complex; there are no low-field resonances for this complex.

complex, and the pK_a of 6.9 is assigned to His 57. The downfield resonance in the complex with phosphonate A titrates with a pK_a value of 3.8 and shows no variation in chemical shift from pH 5.8 to pH 9.0. This resonance is due to the anionic tetrapeptide adduct, and the pK_a represents ionization of the phosphonic acid. The pK_a of His 57 in this complex is most likely raised above 9 by stabilization of the positive charge on the imidazolium ion through hydrogen bonding with the phosphonate. A similar effect has been observed with the negatively charged boronic acid adducts (Bachovchin, 1988) and with the diisopropyl fluorophosphate inhibited enzyme (Porubcan et al., 1979).

Note should be made of the surprisingly large upfield shift of the hexapeptide complex. While a typical phosphonate diester has a chemical shift of 25 ppm in aqueous solution,

the enzyme-bound phosphonate appears between δ 0.83 and δ 3.50, depending on pH. Gorenstein (1989) has reviewed several factors which affect ^{31}P chemical shift which include bond angle effects, stereoelectronic effects, and environmental effects, such as solvent, salt, and ring currents. It would be simplest to invoke environmental effects because the nucleus observed is located in an enzyme active site rather than free in solution. However, the phosphorus of the anionic tetrapeptide complex is in virtually the same magnetic environment, except for the orientation of His 57. Gorenstein et al. (1988) have shown that ring current effects are small and strongly distance dependent. The imidazole of His 57 is approximately 5 Å from the phosphorus atom, a distance at which no ring current effect is expected. It is plausible that because of the binding interactions of the lactylalanyl moiety (P1′–P2′), the ester phophorus atom is bound in a more strained geometry than the acid phosphorus. However, there do not appear to be deviations in bond angles in the crystal structures from simple phophonic acids and ester which exhibit conventional ^{31}P NMR shifts. Furthermore, there are no gross differences in stereoelectronic orientations of the two types of adduct in the crystal structures. Hence, what remains is the unsatisfactory explanation that some or all of these effects are acting simultaneously and additively.

Discussion

Development of activated phosphonate esters that are capable of reacting with the active site Ser in serine proteases to form a stable tetrahedral adduct has allowed, for the first time, study of the structure of an analogue of the high-energy tetrahedral intermediate that occurs when the enzyme becomes acylated by peptide substrates. Enzyme–analogue complexes that have been studied previously, such as boronic acid, fluoro ketone, and aldehyde complexes (Bone et al., 1987, 1989b; Takahashi et al., 1989; R. Bone, C. A. Kettner, and D. A. Agard, unpublished results; James et al., 1980; Brayer et al., 1979a; Delbaere & Brayer, 1985), are most properly analogues of the high-energy intermediate for the deacylation reaction, which is rate limiting for ester hydrolysis but not amide hydrolysis (Hunkapiller et al., 1976). For the P_5–P_1 residues of the inhibitor, the inhibitor conformation, structural changes induced in the enzyme, and enzyme–inhibitor interactions are all nearly identical for the structure of the phosphonate complex determined in this work and for the structures of peptidyl boronic acids (Figure 3) and peptidyl aldehydes. The largest conformational change, the His 57 side-chain rotation, is very localized (Figure 3) and does not affect the utility of using these phosphonate complexes as models for the transition state. Conclusions drawn previously from the study of the structures of complexes which lack P′ substituents remain valid and apply toward understanding the transition state for the acylation reaction.

Two aspects of the structure are quite remarkable and bear some discussion. First, addition of the P_1' and P_2' residues induces no changes in the structure of the enzyme beyond changes induced by analogues lacking these substituents (Figure 3). Extension of the peptide chain to the P_1' and P_2' residues allows the enzyme to form two additional hydrogen bonds (Figure 2) upon complex formation and to remove 120 Å^2 more hydrophobic surface from solvent (Table II by comparison with phosphonate A). With solvent exclusion from hydrophobic surfaces generating 0.025 kcal mol^{-1} Å^{-2} (Richards, 1977) and hydrogen bonds contributing an estimated 1.5–3 kcal/H-bond (Fersht et al., 1985b), addition of these two residues would be expected to contribute an additional 6–9 kcal toward the enzyme–inhibitor interaction energy. Similar energetic contributions would be expected during substrate hydrolysis since this enzyme–inhibitor complex resembles closely the transition state for peptide bond hydrolysis. However, only 2.3 kcal/mol improvement in k_{cat}/K_M is actually realized when Ac-Pro-Ala-Pro-Ala-NH_2 is extended to Ac-Pro-Ala-Pro-Ala-Ala-Ala-NH_2 (Delbaere et al., 1981).

Several factors may be involved in attenuating the actual contribution of the P_1' and P_2' residues toward substrate hydrolysis. In complexes between α-lytic protease and boronic acids, a molecule of solvent, which appears to be sequestered by the carbonyl of Leu 41, contributes an extra hydrogen bond to the hydroxyl of the boronic acid that fills the oxyanion binding pocket. As previously noted (Bone et al., 1987), this interaction may stabilize the transition state for the cleavage of peptide substrates without P′ residues and is lost when substrates with P′ residues interact with the enzyme. Therefore, the observed effect of adding an Ala-amide to the C-terminus of the substrate (1.4 kcal) may be attenuated. In addition, the nearly gauche conformation of the P_1' carbonyl and ester oxygens is a high-energy configuration that must detract from the net $\Delta\Delta G$ for adding the P_1' residue.

Perhaps the most surprising aspect of these studies is the observation that His 57 rotates away from its native position and does not hydrogen bond with the phosphonate ester oxygen. While a neutral His would be prohibited from occupying its native position on steric grounds, a positively charged His should be able to hydrogen bond with the phosphonate ester oxygen as it does when the ester has been cleaved (occupancy A, phosphonate A complex; Figure 7). The low-pH crystallographic experiments effectively rule out the possibility that the pK of His 57 had shifted sufficiently to maintain an uncharged histidine. Because of the phosphonate ester oxygen in occupancy B (phosphonate A complex) and its equivalent in occupancy A lie only 0.1 Å apart, there appears to be no steric explanation for the absence of this hydrogen bond.

Rotation of the imidazolium side chain out of the active site cleft appears to be correlated with the absence of charge in or near the oxyanion pocket. The His rotation occurs in other serine protease–inhibitor complexes in which His 57 is positively charged, and there is no negative charge in or near the oxyanion pocket, such as complexes with peptide aldehydes (R. Bone, C. A. Kettner, and D. A. Agard, unpublished results; James et al., 1980; Brayer et al., 1979a) or sulfonic acids (Bachovchin, 1986). In contrast, in complexes of serine proteases with compounds which have a negative charge in or near the oxyanion pocket, such as peptide boronic acids (Bone et al., 1987; Bachovchin et al., 1988), peptide reaction products (R. Bone, C. A. Kettner, and D. A. Agard, unpublished results; James et al., 1980) and fluoro ketones (Takahashi et al., 1989; Brady et al., 1989), the positively charged His remains in the active site cleft and hydrogen bonds to Asp 102 and to the ligand. Furthermore, in crystals of free α-lytic protease the positively charged His remains rotated into the active site where it ineracts with a negatively charged sulfate that projects into the oxyanion hole (Fujinaga et al., 1985; Brayer et al., 1979a).

The inability of the His to interact productively with the uncharged phosphonate ester provides further evidence that the enzyme has evolved an electrostatic environment that can stabilize an anionic tetrahedral intermediate, as has been suggested by Washel (Washel et al., 1989; Hwang & Washel, 1987). In complexes with charged reaction intermediates a pattern of negative–positive–negative–positive dipoles (Asp 102–His 57–P_1 oxyanion–oxyanion hole) is established and stabilized. If the charge distribution in an analogue of this

intermediate is not anionic, the enzyme evidently cannot respond properly, and the His side chain is expelled from the active site.

Because crystallographic studies require weeks, deviations must exist between the structure of the transition-state complex and the structures of complexes with stable analogues of the transition state. Complexes of serine proteases with peptidyl boronic acids are excellent analogues of the high-energy tetrahedral intermediates that occur during peptide bond hydrolysis (Bone et al., 1987). However, the charge distribution about the boron and the absence of P′ residues must be considered when conclusions from these structures regarding the structure of the transition state are drawn (Bone et al., 1989b). In the complex of α-lytic protease with irreversibly bound phosphonate B, the charge distribution about the phosphorus does not match that of the transition state, though P_1' and P_2' residues are present. As stated above, it may be this deviation from the transition-state structure, combined with deviations in bonds and bond angles about the phosphorus, that leads to the expulsion of His 57 from the active site cleft. Although the histidine rotation would not be expected to occur during the transition state for peptide bone hydrolysis, this conformational change is very well localized and other interactions between the phosphonate and the enzyme would be expected to mimic interactions of the enzyme with the high-energy intermediate that occurs during acylation of the enzyme by substrates. Furthermore, it should be possible to obtain a rather close estimate for the position of the histidine in the transition state by using the location found in the peptidyl boronic acids or with the cleaved phosphonate.

How does the structure of an analogue of the transition state for acylation compare with the structure of an analogue of the Michaelis complex complete with P and P′ residues? The structure of the most similar Michaelis complex is that of the complex formed between *S. griseus* protease B, a bacterial homologue of α-lytic protease, and the third domain of turkey ovomucoid (Read et al., 1983; Fujinaga et al., 1982; Sielecki et al., 1979). The active site of this enzyme–inhibitor complex with the residues of the ovomucoid that fill substrate recognition sites S_5–S_2' is shown in Figure 7 and was obtained from the Brookhaven Data Bank. Comparison of Figures 2 and 4 shows that the main-chain conformations of the phosphonate ester and the protein inhibitor are nearly identical. No bond is formed between the protein inhibitor and the active site serine, and the carbonyl is levered away from Ser 195 and His 57 (Table III). Although many interactions stabilize protease–protein inhibitor complexes besides those shown in Figure 4, they are the ones that are equivalent to interactions in the phosphonate ester complex. Most significant is the observation that one hydrogen bond is lost, that between the carbonyl of Ser 214 and the amide of the P_1 residue, and that one hydrogen bond is stretched, between the P_1 carbonyl oxygen and the amide of Ser 195, in the Michaelis-like complex (Table III). Similar observations have been made during structural studies of subtilisin (Robertus et al., 1972) and *S. griseus* protease A (James et al., 1980). Observations on several different systems (Robertus et al., 1982; James et al., 1980; R. Bone, C. A. Kettner, and D. A. Agard, unpublished results) indicate that not all hydrogen bonds formed in complexes between enzyme and transition-state analogues are formed in the corresponding complexes with substrate analogues. Furthermore, which hydrogen bonds are left unmade can vary from complex to complex.

For α-lytic protease it appears that the transition state differs from the Michaelis complex by the development of charge on the P_1 carbonyl oxygen, by improvement of the hydrogen bond it makes with the NH of Ser 195, and by the gain of a single hydrogen bond. In the Michaelis complex, binding energy is being used to sequester the reactant from solvent and maintain it in a transition-state-like position, a process whereby unfavorable consequences of binding are slightly more than compensated for by the energy gained from intermolecular interaction. However, one or a few potential interactions are not satisfied in this ground-state complex and can only be satisfied by transformation toward the transition state. These interactions exist as potential interactions, neither formed nor able to interact with solvent, and only upon reaching the transition state are their full energies realized.

Formation of a hydrogen bond with a charged partner in the vapor phase has been estimated to have an energy of up to 18 kcal/mol (Weiner et al., 1984). On the basis of recent calculations (Mitchell & Price, 1990; Cybilski & Schieiner, 1989) the improvement in a hydrogen-bond length by 0.3 Å might be expected to translate into up to 1.8 kcal/mol of transition-state stabilization. In the Michaelis complex the hydrogen-bonding partners have been desolvated and restricted conformationally so that when the hydrogen bond is actually formed in the transition-state complex there should be very little further loss of entropy. The full enthalpy of hydrogen-bond formation should be realized as a result of this transformation with almost no loss in entropy and may exceed the value of 6 kcal/mol for the formation of a vapor-phase hydrogen bond (Weiner et al., 1984). Coulombic interactions introduced upon formation of an ion pair between positively charged His 57 and the anionic intermediate should also liberate energy (Brady et al., 1989; Washel et al., 1989). For peptide bond hydrolysis by serine proteases it appears that the sum of these interactions produces as much as 12–14 kcal/mol stabilization energy (Carter & Wells, 1988) as the system approaches the transition state.

References

Alden, R. A., Birktoft, J. J., Kraut, J., Robertus, J. D., & Wright, C. S. (1971) *Biochem. Biophys. Res. Commun. 45*, 337.

Bachovchin, W. W. (1986) *Biochemistry 25*, 7751–7759.

Bachovchin, W. W., Wong, W. Y. L., Farr-Jones, S., Shenvi, A. B., & Kettner, C. A. (1988) *Biochemistry 27*, 7688.

Blevins, R. A., & Tulinski, A. (1985) *J. Biol. Chem. 260*, 4264.

Blow, D. M. (1976) *Acc. Chem. Res. 9*, 145.

Bode, W., Paparokos, E., & Musil, D. (1987) *Eur. J. Biochem. 166*, 673.

Bode, W., Meyer, E., Jr., & Powers, J. C. (1989) *Biochemistry 28*, 1951–1963.

Bone, R., Shenvi, A. B., Kettner, C. A., & Agard, D. A. (1987) *Biochemistry 26*, 7609–7614.

Bone, R., Silen, J. L., & Agard, D. A. (1989a) *Nature 339*, 191–195.

Bone, R., Frank, D., Kettner, C. A., & Agard, D. A. (1989b) *Biochemistry 28*, 7600–7609.

Brady, K., Liang, T.-C., & Abeles, R. H. (1989) *Biochemistry 28*, 9066–9070.

Brayer, G. D., Delbaere, L. T. J., & James, M. N. G. (1978a) *J. Mol. Biol. 124*, 243–259.

Brayer, G. D., Delbaere, L. T. J., & James, M. N. G. (1978b) *J. Mol. Biol. 124*, 261–283.

Brayer, G. D., Delbaere, L. T. J., James, M. N. G., Bauer, C. A., & Thompson, R. C. (1979a) *Proc. Natl. Acad. Sci. U.S.A. 76*, 96–100.

Brayer, G. D., Delbaere, L. T. J., & James, M. N. G. (1979b) *J. Mol. Biol. 131*, 743–775.

Carter, P., & Wells, J. A. (1988) *Nature 332*, 564–568.
Chambers, J. L., & Stroud, R. M. (1977) *Acta Crystallogr., Sect. B 33*, 1824–1837.
Connolly, M. L. (1983a) *J. Appl. Crystallogr. 16*, 548–558.
Connolly, M. L. (1983b) *Science 221*, 709–713.
Cybilski, S. M., & Schieiner, S. (1989) *J. Phys. Chem. 93*, 6565–6574.
Delbaere, L. T. J., & Brayer, G. D. (1980) *J. Mol. Biol. 139*, 45–51.
Delbaere, L. T. J., & Brayer, G. D. (1985) *J. Mol. Biol. 183*, 89–103.
Delbaere, L. T. J., Brayer, G. D., & James, M. N. G. (1981) *Eur. J. Biochem. 120*, 289–294.
Drenth, J., Hol, W. G. J., Jansonius, J. N., & Koekoek, R. (1972) *Eur. J. Biochem. 26*, 177.
Fersht, A. (1985a) *Enzyme Structure and Mechanism*, 2nd Ed., Freeman, San Francisco.
Fersht, A. R., Shi, J.-P., Knill-Jones, J., Lowe, D. M., Wilkinson, A. J., Blow, D. M., Brick, P., Carter, P., Wayne, M. M. Y., & Winter, G. (1985b) *Nature 314*, 235–238.
Fujinaga, M., Read, R., Sielecki, A. R., Ardelt, W., Laskowski, M., Jr., & James, M. N. G. (1982) *Proc. Natl. Acad. Sci. U.S.A. 79*, 4868–4872.
Fujinaga, M., Delbaere, L. T. J., Brayer, G. D., & James, M. N. G. (1985) *J. Mol. Biol. 183*, 479–502.
Fujinaga, M., Sielecki, A. R., Read, R. J., Adelt, W., Laskowski, M., Jr., & James, M. N. G. (1987) *J. Mol. Biol. 195*, 397.
Furey, W. J. (1984) in *Methods and Applications in Crystallographic Computing* (Hall, S. R., & Ashida, T., Eds.) pp 352–371, Clarendon, Oxford, England.
Gorenstein, D. G. (1989) *Methods Enzymol. 177*, 295–316.
Gorenstein, D. G., Schroeder, S. A., Fu, J. M., Metz, J. T., Roongtu, V., & Jones, C. R. (1988) *Biochemistry 27*, 7223–7237.
Hames, B. D., & Rickwood, D., Eds. (1981) *Gel Electrophoresis of Proteins*, IRL, Oxford, England.
Hendrickson, W. A., & Konnert, J. (1981) in *Biomolecular Structure, Function, Conformation, and Evolution* (Srinivasam, R., Ed.) Vol. 1, pp 43–47, Pergamon, Oxford, U.K.
Hunkapiller, M. W., Smallcombe, S. H., Whitaker, D. R., & Richards, J. H. (1973) *Biochemistry 12*, 4732–4743.
Hunkapiller, M. W., Forgac, M. D., & Richards, J. H. (1976) *Biochemistry 15*, 5581–5588.
Hwang, J.-K., & Washel, A. (1987) *Biochemistry 26*, 2669–2673.
Imperiali, B., & Abeles, R. H. (1986) *Biochemistry 25*, 3760–3767.
James, M. N. G., Sielecki, A. R., Brayer, G. D., Delbaere, L. T. J., & Bauer, C. A. (1980) *J. Mol. Biol. 144*, 43–88.
Jones, T. A. (1982) in *Computational Crystallography* (Sayre, D., Ed.) pp 303–317, Oxford University, Oxford, England.
Kettner, C. A., & Shenvi, A. B. (1984) *J. Biol. Chem. 259*, 15106–15114.
Kettner, C. A., Bone, R., Agard, D. A., & Bachovchin, W. W. (1988) *Biochemistry 27*, 7682–7688.
Krieger, M., Chambers, J. L., Christoph, G. G., & Stroud, R. M. (1974) *Acta Crystallogr., Sect. A 30*, 740–748.
Marquart, M., Walter, J., Deisenhofer, J., Bode, W., & Huber, R. (1983) *Acta Crystallogr., Sect. B 39*, 480.
Matthews, D. A., Alden, R. A., Birktoft, J. J., Freer, S. T., & Kraut, J. (1975) *J. Biol. Chem. 250*, 7120–7126.
McPhalen, C. A., & James, M. N. G. (1988) *Biochemistry 27*, 6582–6598.
Meyer, E. F., Jr., Radhakrishnan, R., Cole, G. M., & Presta, L. G. (1986) *J. Mol. Biol. 189*, 533–539.
Meyer, E. F., Cole, G. M., Radahakrishnan, R., & Epp, O. (1988) *Acta Crystallogr., Sect. B 44*, 26.
Mitchell, J. B. O., & Price, S. L. (1990) *J. Comput. Chem. 11*, 1217–1233.
Porubcan, M. A., Westler, W. M., Ibanez, I. B., & Markley, J. L. (1979) *Biochemistry 18*, 4108–4116.
Read, R. J., & James, M. N. G. (1988) *J. Mol. Biol. 200*, 523.
Read, R. J., Fujinaga, M., Sielecki, A. R., & James, M. N. G. (1983) *Biochemistry 22*, 4420–4433.
Richards, F. M. (1977) *Annu. Rev. Biophys. Bioeng. 6*, 151–176.
Robertus, J. D., Kraut, J., Alden, R. A., & Birktoft, J. J. (1972) *Biochemistry 11*, 4293–4303.
Sampson, N. S., & Bartlett, P. A. (1988) *J. Org. Chem. 53*, 4500–4503.
Sampson, N. S., & Bartlett, P. A. (1991) *Biochemistry* (preceding paper in this issue).
Schecter, I., & Berger, A. (1967) *Biochem. Biophys. Res. Commun. 27*, 157.
Sielecki, A. R., Hendrickson, W. A., Broughton, C. G., Delbaere, L. T. J., Brayer, G. D., & James, M. N. G. (1979) *J. Mol. Biol. 134*, 781.
Silen, J. L., Frank, D., Fujishige, A., Bone, R., & Agard, D. A. (1989) *J. Bacteriol. 171*, 1320–1325.
Smith, J. L., Corfield, P. W. R., Hendrickson, W. A., & Low, B. W. (1988) *Acta Crystallogr., Sect. A 44*, 357–368.
Stroud, R. M., Kieg, L. J., & Dickerson, R. E. (1974a) *J. Mol. Biol. 83*, 185.
Stroud, R. M., Kay, L. M., & Dickerson, R. E. (1974b) *J. Mol. Biol. 83*, 185–208.
Takahashi, L. H., Radhakrishnan, R., Rosenfield, R. E., Meyer, E. F., & Trainor, D. A. (1989) *J. Am. Chem. Soc. 111*, 3368–3374.
Thompson, R. C. (1973) *Biochemistry 12*, 47–51.
Tsukada, H., & Blow, D. M. (1985) *J. Mol. Biol. 184*, 703.
Tulinsky, A., & Blevins, R. A. (1987) *J. Biol. Chem. 262*, 7737–7743.
Walter, J., Steigemann, W., Singh, T. P., Bartunik, H., Bode, W., & Huber, R. (1982) *Acta Crystallogr., Sect. B 38*, 1462.
Washel, A., Naray-Szabo, G., Sussman, F., & Hwang, J.-K. (1989) *Biochemistry 28*, 3629–3637.
Weiner, S. J., Kollman, P. A., Case, D. A., Singh, U. C., Ghio, C., Alagona, G., Profeta, S., & Weiner, P. (1984) *J. Am. Chem. Soc. 106*, 765–784.
Whitaker, D. R. (1970) *Methods Enzymol. 19*, 599–613.
Wycoff, H. W., Dorscher, R., Tsernoglou, D., Inagami, T., Johnson, L., Hrdman, K. D., Allewell, N. M., Kelly, D. M., & Richards, F. M. (1967) *J. Mol. Biol. 27*, 563–578.